Theor Chem Acc (2005) 113: 274–280
DOI 10.1007/s00214-005-0668-6

REGULAR ARTICLE

P. Homem-de-Mello · B. Mennucci
J. Tomasi · A. B. F. da Silva

The effects of solvation in the theoretical spectra of cationic dyes

Received: 28 October 2004 / Accepted: 3 March 2005 / Published online: 23 May 2005

Abstract We present a quantum-mechanical study on the solvent effects in the structure and electronic spectra of some cationic dyes: acridine orange, proflavine, safranine, neutral red, thionine and methylene blue. The geometry optimizations were carried out with the AM1 and DFT (with B3LYP functional) methods and the theoretical spectra of the dyes under study were obtained with ZINDO and time-dependent methods (TD–DFT and TD–HF). The solvation methodology adopted was the integral equation formulation (IEF) version of the polarizable continuum model (PCM).

Keywords Cationic dyes · ZINDO · Time-dependent calculations · IEF-PCM

1 Introduction

Historically, the initial development of dyes can be traced back to their use in the textile industry although later developments extended their utilization to other important applications such as photography, medicine, biology, food industry, cosmetics, analytical chemistry and others. In the specific case of cationic dyes, the first applications were related to the dyeing of cotton, leather and paper [1,2].

Some of these dyes possess bacteriostatic and antibacterial activity and due to their active absorption by animal tissues they have been largely used as dye staining submolecular particles. Dyes have been also studied for their interactions with biological systems as the dyes spectra are modified when bound to acidic structures (or present in acidic compartments). Therefore, dyes are very useful in histology to stain nucleic acids, chromatin and lysosomes. The dye neutral red was found to inhibit the growth of carcinoma; proflavine has important antiseptic properties; methylene blue photoinactivate viruses and, as thionine, in combination with visible light, can be used to decontaminate fresh plasma [3–6].

Cationic dyes can also be employed as analytical reagents for gravimetric and titrimetric determination of metal cations and inorganic anions, as acid base indicators or even as color-development reagents for spectrophotometric and fluorimetric determinations, photokinetic indicators, luminescence sensors or reagents for drug analysis. A variety of cationic dyes have been successfully incorporated in other materials and have been utilized, for example, in photodegradation of organic pollutants, in electrocatalysis, as electrochromic devices, in solar cells and as biosensors [7–11].

Nowadays, cationic dyes are also being used as probes in the study of microheterogeneous and biological systems (clays, micelles, vesicles, microemulsions, DNA and nucleosides) [1,2,12–15]. This is based on their photophysical and photochemical properties, which strongly depend on the nature of the surrounding environment. All these applications demonstrate the importance of the study of cationic dyes, particularly to determinate their photophysical and photochemical properties.

During the last five decades, the Pariser-Parr-Pople (PPP) method [16], the semi-empirical CNDO/S method [17] and the ZINDO method [18,19] have been employed to predict the absorption characteristics of dyes [20]. Recently, Guillaumont and Nakamura used the time-dependent density functional theory (TD–DFT) for the calculation of excitation energies and oscillator strengths for some organic dyes [21]. In that study, they observed that the TD–DFT method reproduced correctly the experimental data of the molecules studied, but for the cationic dye studied the difference between the experimental and the calculated values was larger. This difference was attributed to the flexible structure of the cationic dye, which could lead to several conformations in solution.

P. Homem-de-Mello · A. B. F. da Silva (✉)
Grupo de Química Quântica,
Departamento de Química e Física Molecular,
Instituto de Química de São Carlos,
Universidade de São Paulo - Cx. Postal 780,
13560-970 São Carlos, Brazil
E-mail: alberico@iqsc.usp.br

B. Mennucci · J. Tomasi
Dipartimento di Chimica e Chimica Industriale,
Università di Pisa, Via Risorgimento 35,
56122 Pisa, Italy

Commonly, solvation effects can be included in calculation with a continuum or a discrete description of the solvent. The distinctive advantages of continuum methods are the consistence and relative simplicity of their physical foundations [22]. A well-known continuum approach is the integral equation formulation (IEF) [23] version of the polarizable continuum model (IEF-PCM) [24], which is able to give an accurate description of the electrostatic interaction between the solute and the solvent modeled in terms of an apparent surface charge spread on a cavity of molecular shape.

Aiming at determining the role of solvent on structural and electronic properties, as well as on absorption spectra, we have chosen for this work a set of cationic dyes, namely: acridine orange (AO), proflavine (PF), safranine (SF), neutral red (NR), methylene blue (MB) and thionine (TN). These dyes have been studied with different quantum mechanical (QM) methods, in gas-phase and in aqueous solution. In particular, we used AM1 and DFT methods to obtain the equilibrium geometries and ZINDO, TD–DFT and TD–HF methods to compute the absorption energies.

2 Computational methods

The set of cationic dyes studied in the present work can be grouped into three families: thiazines (MB and TN), acridines (AO and PF) and diazines (NR and SF). The chemical structures of the dyes studied, along with the cartesian axes adopted in this work, are presented in Fig. 1.

The molecules were optimized with the AM1 [25] and DFT [26] methods in gas-phase and in solution, providing, consequently, four different geometries for each dye. Among the cationic dyes studied we have selected two, MB and AO, to evaluate the best methodology. On these two selected systems, we have performed ZINDO, time-dependent Hartree Fock (TD–HF) and TD–DFT [27] calculations using the four structures previously obtained (two in gas-phase and two in solution). The spectra of the other four cationic dyes were calculated with ZINDO in gas-phase and in solution. In fact, as shown in the next section, the spectra obtained for MB and AO with ZINDO are in excellent agreement with the experimental data, and for this reason the ZINDO method was chosen to calculate the absorption spectra of PF, TN, NR and SF instead of the much more time-consuming TD–HF and TD–DFT methods.

All the calculations were performed with a local version of the Gaussian 03 code [28]. The HF calculations were carried out using the 6-31+G(d) basis set [29] and the DFT calculations made use of the B3LYP functional [30] with the 6-31+G(d) basis set.

The solvent (water) effect was always simulated in the calculations through the IEF–PCM method. Here, we do not report the details of the IEF–PCM approach and of its generalization to TD–HF(DFT) and ZINDO methods, but we refer the readers to the related papers, namely [31] and [32]. The only aspect which we would like to recall is that the transition energy estimated by IEF–PCM refers to a vertical transition, and this means that the explicit solvent effect on the transition energy is determined only by the electronic part of the solvent. In the general IEF–PCM approach, solute electronic and nuclear charge distribution and solvent reaction field mutually equilibrate. When a sudden change in the solute electronic density occurs, as during an electronic transition, such equilibrium condition between the solute and the solvent is no longer valid, as the relaxation of the reaction field in the direction of the new solute electronic state may be incomplete. If we take into account the typical time scales characterizing electronic and nuclear (or molecular) motions, we can safely assume that only the part of the solvent reaction which is induced by the polarization of its electrons can immediately modify according to the new electronic state reached by the solute in the transition process; all the rest remains frozen in the previous equilibrium condition determined by the initial state [33].

The cavity in which the solute is embedded is obtained as a superposition of overlapping spheres centered on heavy atoms defined in terms of van der Waals radii [34] multiplied by a factor ($f = 1.2$) [22]: only the hydrogen atoms bonded to nitrogen have their proper sphere. The resulting radii we have used are 2.40 for –CH_3, 2.28 for –CH, 2.04 for –C, 1.92 for –N, 1.44 for –H bonded to N and 2.16 for –S.

3 Results and discussion

The optimizations performed with the AM1 and DFT methods led to planar molecular structures for all the cationic dyes studied with the exception of the SF dye, whose phenylic ring is found to be perpendicular to the plane of the rest of the molecule (we have adopted the xy plane as the molecular plane, see Fig. 1).

In order to verify if the equilibrium position of the phenylic ring was really 90°, we carried out other optimizations in gas-phase and in solution initially placing the phenylic ring in the same plane of the rest of the molecule and making a careful conformation analysis varying the twisting angle. The results for this analysis confirmed the same final structure obtained when we started the optimization with the phenylic ring in a perpendicular position to the rest of the molecule.

As expected from the rigid structures of these dyes, both at AM1 and DFT level, the differences found in the optimized geometries in gas-phase and in solution are small. These minor structural differences appear mainly around the heteroatom of the central ring. Table 1 presents some of the geometrical parameters of this region of the dye molecules: the bond length between the heteroatom and a carbon atom (S–C bond for MB and TN, N–C bond for the other dyes), the distance between two carbons bonded to the heteroatom and the angle formed by these two carbons and the heteroatom.

The structures obtained in solution have the angle C–X–C (X = heteroatom) smaller than the respective angle for the structures obtained in gas-phase, except the SF dye whose angle becomes larger when optimized in solution. If the C–X–C

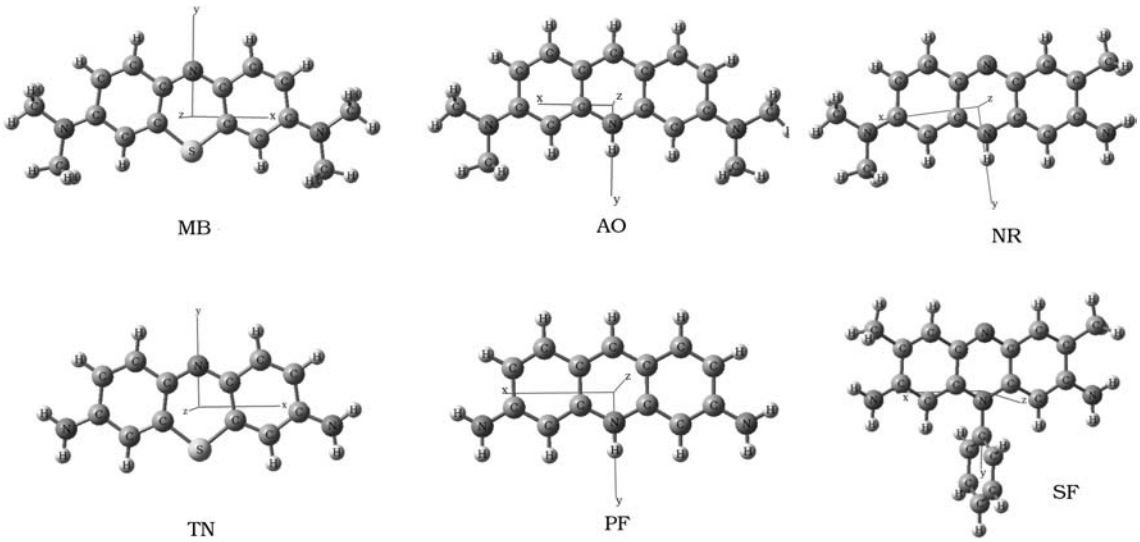

Fig. 1 Structures of the cationic dyes studied and the cartesian orientation adopted in this work

Table 1 Selected geometrical parameters for the cationic dyes studied obtained at two different levels of calculation in gas-phase (*g*) and in solution (w)

Dye	Geometry	C–X* (Å)	C–C (Å)	C–X–C (°)
MB	AM1 (g)	1.659	2.631	104.880
	AM1 (w)	1.650	2.613	104.774
	DFT (g)	1.751	2.746	103.297
	DFT (w)	1.751	2.744	103.227
AO	AM1 (g)	1.385	2.425	122.273
	AM1 (w)	1.382	2.417	121.992
	DFT (g)	1.377	2.444	125.136
	DFT (w)	1.374	2.437	124.884
TN	AM1 (g)	1.657	2.626	104.852
	AM1 (w)	1.653	2.620	104.793
	DFT (g)	1.747	2.740	103.295
	DFT (w)	1.748	2.740	103.240
PF	AM1 (g)	1.384	2.423	122.222
	AM1 (w)	1.382	2.418	122.010
	DFT (g)	1.375	2.441	125.091
	DFT (w)	1.373	2.435	124.888
NR	AM1 (g)	1.383	2.408	121.014
	AM1 (w)	1.379	2.402	120.897
	DFT (g)	1.372	2.417	123.425
	DFT (w)	1.368	2.410	123.318
SF	AM1 (g)	1.391	2.412	120.239
	AM1 (w)	1.391	2.414	120.365
	DFT (g)	1.384	2.410	121.061
	DFT (w)	1.384	2.411	121.187

*X = S for MB and TN and N for the other dyes

Table 2 Wavelength (λ_{max} in nm) for MB in gas-phase (g) and in solution (w) calculated at TD–HF, TD–DFT and ZINDO level at four different geometries

Geometry	Spectrum	λ_{max} (nm)	Error* (%)
AM1 (g)	ZINDO (g)	581.0	11
	ZINDO (w)	640.5	2
	TD–HF (g)	423.8	35
	TD–HF (w)	448.1	32
	TD–DFT (g)	512.2	22
	TD–DFT (w)	541.3	18
AM1 (w)	ZINDO (g)	579.5	12
	ZINDO (w)	636.4	3
	TD–HF (g)	421.3	36
	TD–HF (w)	444.2	32
	TD–DFT (g)	513.9	22
	TD–DFT (w)	542.5	17
DFT (g)	ZINDO (g)	582.2	11
	ZINDO (w)	649.4	1
	TD–HF (g)	432.5	34
	TD–HF (w)	462.2	30
	TD–DFT (g)	500.7	24
	TD–DFT (w)	531.3	19
DFT (w)	ZINDO (g)	583.2	11
	ZINDO (w)	651.3	1
	TD–HF (g)	433.1	34
	TD–HF (w)	463.2	30
	TD–DFT (g)	500.9	24
	TD–DFT (w)	531.7	19

*Error (%) corresponds to the difference between the calculated λ_{max} and the experimental value in aqueous solution (657 nm [2, 14])

angle becomes smaller, the heteroatom (X) is more exposed to the solvent, making possible the interaction heteroatom-solvent and the stabilization of the solute. The SF dye is the only exception because in this molecule there is a phenylic ring bonded to the heteroatom, and this makes this region of the molecule more hydrofobic.

As mentioned before, we performed a preliminary study of the excitation energies for the MB and AO dyes by employing three different QM methods, TD–HF, TD–DFT and ZINDO. The results of this study for MB and AO are reported in Tables 2 and 3, respectively. For each dye, we computed the excitation energies both in gas-phase and in solution at the four different structures previously obtained. In Tables 2 and 3, the corresponding wavelengths (λ_{max}) are reported together with the error (%) with respect to the experimental values measured in aqueous solution.

Table 3 Wavelength (λ_{max} in nm) for AO in gas-phase (g) and in solution (w) calculated at TD–HF, TD–DFT and ZINDO level at four different geometries

Geometry	Spectrum	λ_{max} (nm)	Error[a] (%)
AM1 (g)	ZINDO (g)	455.5	7
	ZINDO (w)	456.6	7
	TD–HF (g)	334.6	32
	TD–HF (w)	337.7	31
	TD–DFT (g)	440.6	10
	TD–DFT (w)	451.0	8
AM1 (w)	ZINDO (g)	454.1	7
	ZINDO (w)	454.1	7
	TD–HF (g)	333.6	32
	TD–HF (w)	336.3	31
	TD–DFT (g)	441.7	10
	TD–DFT (w)	451.7	8
DFT (g)	ZINDO (g)	452.8	8
	ZINDO (w)	456.1	7
	TD–HF (g)	332.6	32
	TD–HF (w)	336.9	31
	TD–DFT (g)	432.3	12
	TD–DFT (w)	443.8	9
DFT (w)	ZINDO (g)	452.3	8
	ZINDO (w)	455.2	7
	TD–HF (g)	332.2	32
	TD–HF (w)	336.3	31
	TD–DFT (g)	432.9	12
	TD–DFT (w)	444.1	9

[a]Error (%) corresponds to the difference between the calculated λ_{max} and the experimental value in aqueous solution (490 nm [15])

Table 4 Wavelength (ZINDO λ_{max} in nm) for NR, SF, TN and PF in gas-phase and in solution calculated at different DFT geometries

Dye	Geometry	Spectrum	λ_{max} (nm)	Error[a] (%)	λ_{exp} (nm)
PF	g	g	428.7	4	445
	g	w	441.6	1	
	w	g	428.8	4	
	w	w	441.6	1	
TN	g	g	549.9	8	600
	g	w	628.0	5	
	w	g	551.7	8	
	w	w	631.1	5	
NR	g	g	519.6	3	535
	g	w	555.0	4	
	w	g	519.8	3	
	w	w	555.0	4	
SF	g	g	503.7	5	530
	g	w	551.3	4	
	w	g	505.2	5	
	w	w	553.8	5	

w calculation performed including the solvent (water) and *g* calculation performed in gas-phase

[a]Error (%) corresponds to the difference between the calculated λ_{max} and the experimental value (λ_{exp} [2, 14])

The calculated λ_{max} presented error of approximately 35% for both MB and AO when computed at TD–HF level, 20% for MB and 10% for AO at TD–DFT level, and less than 10% for MB and AO with the ZINDO method. Taking into account the solvent, the error in the calculated λ_{max} decreased 5% at the TD–HF and ZINDO level and 2% at the TD–DFT level.

This analysis led us to choose the ZINDO method as the selected method to study the absorption spectra of the other dyes in gas-phase and in solution. As expected by the rigid structures of the dyes, the influence of the geometry in spectra is small; however, for both MB and AO systems, DFT geometries give slightly better results and thus we have chosen this method to obtain the geometries of the other dyes. Obviously, this choice can be done here as the dimensions of all the dyes are still computationally tractable at this level; for larger systems, in fact, AM1 would surely be the only possible choice. It is, however, interesting to stress that the results on these two dyes seem to show that AM1 can indeed correctly reproduce the same geometrical parameters found at the by far more accurate DFT level, and thus it can be reliably used for further studies on larger dyes.

In Table 4, we report the ZINDO results, both in gas-phase and in solution, for the dyes PF, TN, NR and SF. For each dye, we have repeated the DFT calculations at two different geometries corresponding to gas-phase and solution.

As we have observed for MB and AO, the IEFPCM–ZINDO results present a better agreement with experiments with respect to the gas-phase analogs; only for NR we found a small increase in the error passing from gas-phase to IEF–PCM results.

In addition to the comments we have made on the results reported in the previous tables, we note here that the two diazine molecules (NR and SF) have experimental absorption maxima with similar wavelengths while in the other two dye families, the smallest molecules (TN and PF, respectively) have their experimental absorption maxima blue-shifted by 50 nm when compared to the other members of the same family. It is useful to recall that the main structural difference between the members of the thiazine and acridine families is the substitution of $-CH_3$ groups in MB and AO, by –H atoms in TN and PF, respectively. From the data reported in Tables 2, 3, 4, it appears evident that this substitution has much smaller effects in the computed excitation wavelengths than in the experimental ones; as a result, dyes belonging to the same family have the calculated absorption maxima closer than in the experimental spectra.

To better understand this finding, we have analyzed the molecular orbitals that mostly contribute to the electronic transition, i.e., the highest occupied molecular orbital (HOMO) and lowest unoccupied molecular orbital (LUMO).

The plots for these molecular orbitals (see Fig. 2) show that the methylic groups in AO and MB have a small contribution to both HOMO and LUMO orbitals: this explains the small differences found in the calculated excitation wavelengths of the two dyes in the same family.

Possibly, the differences experimentally observed in aqueous solution are due to the different solvation of the methyl groups in the larger members with respect to that of the hydrogen atoms in the smaller ones. A possible source of this different solvation is represented by specific interactions (namely H-bonds) between water molecules and the two more acidic

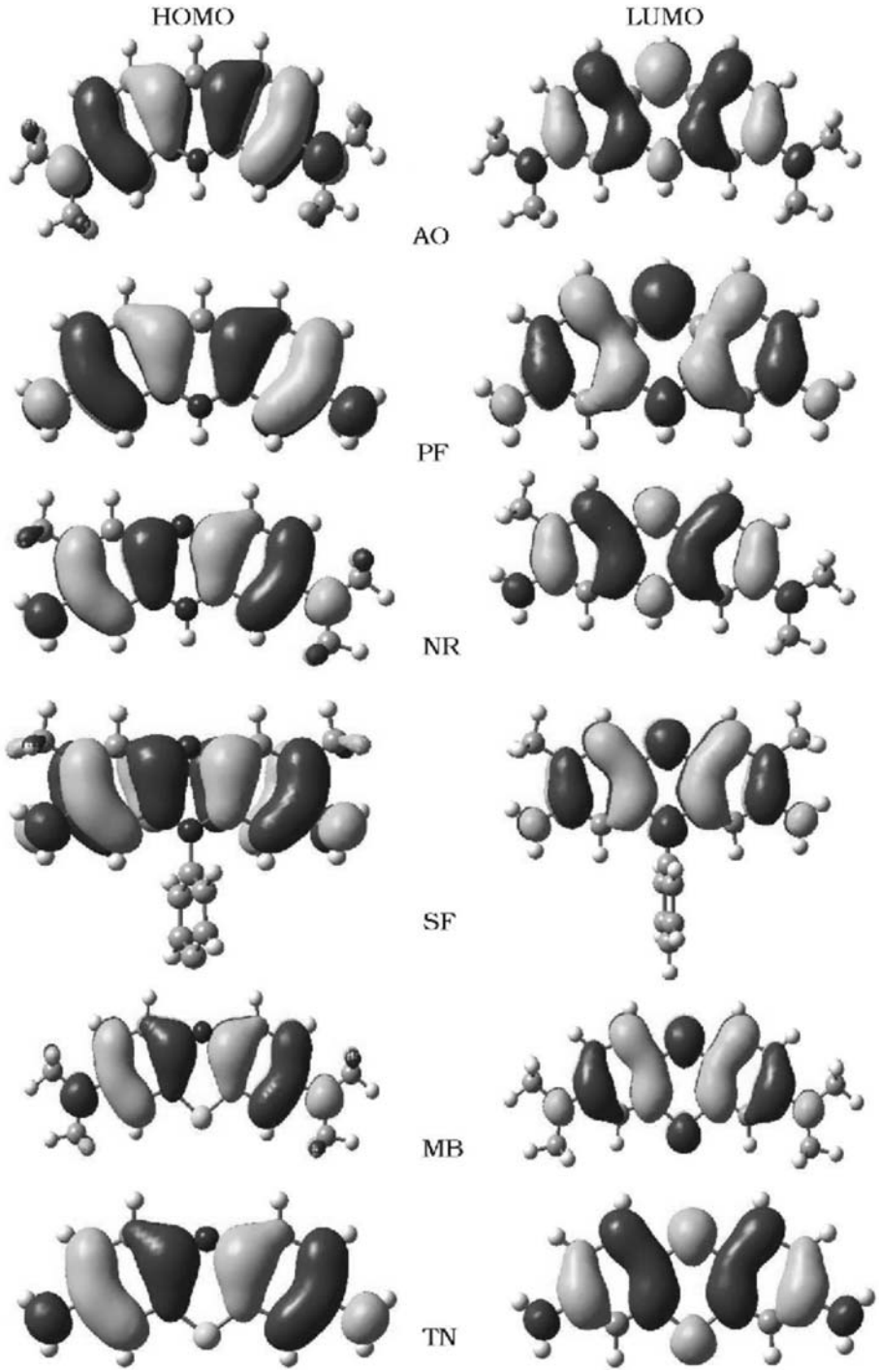

Fig. 2 Highest occupied molecular orbital and Lowest unoccupied molecular orbital plots calculated in solution for the cationic dyes studied

H(N) atoms of PF and TN but not with those of the methyl groups of AO and MB. To analyze this point we have optimized (at DFT level in gas-phase) a cluster of TN with two H-bonded waters (one for each amino group) and we have recalculated the excitation wavelength both in gas-phase and in solution (i.e. adding the external IEF continuum). The λ_{max} we have obtained for these TN-2H_2O clusters (namely 556 nm in gas-phase and 632 nm with IEF), when compared with the corresponding ones calculated without the H-bonded waters (see Table 4), show that the effects of the hydrogen bonds cannot explain the differences between the two members of the family but, by contrast, they make the two systems even more similar. These results, even if limited to a single system and to a single type of cluster, seem to indicate that

Table 5 Difference between excitation energies (in eV) and transition dipole moments (in a.u.) computed at ZINDO level in gas phase (g) and in solution (w). The geometries used are those optimized in the respective phase at DFT level

Dye	Phase	$\Delta\varepsilon_{solv}$ (eV)	μ_x (a.u.)
MB	g	-	5.00
	w	0.23	5.17
TN	g	-	4.65
	w	0.29	4.95
AO	g	-	3.89
	w	0.01	3.97
PF	g	-	3.59
	w	0.08	3.80
NR	g	-	4.17
	w	0.15	4.37
SF	g	-	4.03
	w	0.22	4.38

the differences experimentally observed in the spectra of each family of dyes are more probably originated by differences in the nonelectrostatic part of the solute–solvent interactions and thus extensions of standard continuum models should be introduced.

A more direct analysis of the solvent effect can be obtained in terms of the gas-to-solution shifts. In Table 5, we report these shifts ($\Delta\varepsilon_{solv}$) together with the values of the corresponding transition dipole moments calculated in gas-phase and in solution. All the values reported in Table 5 were computed at the ZINDO level and they refer to geometries optimized in each phase at the DFT level.

The largest solvent shift was found in the two thiazines ($\Delta\varepsilon_{solv}$ is 0.29 eV for TN and 0.23 eV for MB), while the acridines (PF and AO) showed the smallest variation (less than 0.10 eV); the diazines (NR and SF) showed an intermediate shift, 0.15 and 0.22 eV, respectively.

A further analysis of the different solvation effects on the spectra of the dye families studied in this work can be done in terms of the transition dipole moments and their changes with the solvent. Due to the nature of the electronic transition considered here, transition dipole moments are along the x axis (see μ_x in Table 5) except for NR for which there is also a small component along the y axis (around -0.6 a.u.).

In this context, it is interesting to analyze the molecular orbitals involved in the transition and evaluate the relationship between these orbitals and the transition dipole moment. All dyes studied in this work present a spectrum that corresponds to the electronic transition from HOMO to LUMO. The HOMO and LUMO plots indicate from which region of the molecule the electron is excited and the region which this same electron would occupy. For the dyes studied, these plots (Fig. 2) confirmed the direction of the transition dipole moment: their comparison in fact clearly shows that the electronic transition occurs along the longitudinal axis of the molecule, e.g. what we have chosen as the x axis; the asymmetry of NR with respect to the y axis explains the presence of a small component of the transition dipole along this direction.

Passing from the gas-phase to solution, we found an increase in μ_x of 0.17 a.u. for MB, 0.30 a.u. for TN, 0.08 a.u. for AO, 0.20 a.u. for PF and for NR and 0.35 a.u. for SF. We note that family members that have two $-NH_2$ groups bonded to the rings instead of $-N(CH_3)_2$ presented a larger solvent effect on the transition dipole moment: this behavior can be related to larger hydrophilicity of the $-NH_2$ group with respect to $-N(CH_3)_2$, which is reflected in a stronger interaction with the solvent.

4 Conclusions

In this paper, we presented a QM study of the solvent effect on geometries and excitation energies of some cationic dyes. Both methods used to optimize the structures (DFT and AM1), in gas-phase or in aqueous solution, have given nearly planar cationic dyes, except for safranine (SF) in which the phenylic ring is perpendicular to the plane of the rest of the molecule. As expected from the rigid structures of all the cationic dyes studied in this work, our calculations predict small geometrical changes passing from the gas-phase to solution; the few structural differences obtained mainly appear in the bonds and angles involving the heteroatom (X = N or S) of the aromatic cycle. In particular, the solvated dyes present a C–X–C angle smaller than in gas-phase, thus allowing the heteroatom (X) to be more exposed to the solvent; in this way in fact, its electrostatic interaction with the solvent is stronger. The only exception is SF whose phenylic ring bonded to the heteroatom is an obstacle for its interaction with the solvent.

The changes in the geometries originated by the inclusion of the solvent do not cause significant modifications in the absorption spectra, while much more important effects are found when the effect of the solvent is explicitlly accounted for in the calculation of the excitation energies. By accounting for these effects, in fact, the agreement between calculated and experimental spectra significantly improves. Changes in the energy of the frontier molecular orbitals involved in the transition and in the transition dipole moments (μ) are also observed passing from isolated to solvated dyes. The μ values and the molecular orbital plots indicate a charge transfer in longitudinal direction from the more external atoms (those bonded to the extremity rings) to the atoms of the central ring of the molecules.

By computing excitation energies at the ZINDO and TDHF (DFT) level, with DFT and AM1 geometries, we have found that the best agreement with experiments is found at the IEFPCM–ZINDO level with geometries computed at the DFT level. The error for the spectra calculated in solution with the ZINDO method is in fact equal or less than 5% for all dyes with the exception of AO for which the error is slightly larger (7%).

The results of this work clearly indicate the good performance of the DFT (for optimization) and the ZINDO (for theoretical spectra) methods, when combined with the IEF–PCM method, in studying how interactions between solute and

solvent can interfere in the geometry and spectra of cationic dyes.

Acknowledgements The authors thank FAPESP, CAPES and CNPq (brazilian agencies) for the financial support and one of us (P.H.M) thanks FAPESP and CAPES for the scholarships granted.

References

1. Neumann MG, Tiera MJ (1993) Química Nova 16(4):280
2. Neumann MG, Gessner F, Cione APP, Sartori RA, Schimitt CC (2000) Química Nova 23(6):818
3. Aaron JJ, Maafi M, Parkankyi C, Boniface C (1995) Spectrochim Acta 51A(4):603
4. Clerc S, Barenholz Y (1998) Anal Biochem 259:104
5. Mohr H (2001) Transfus Apheresis Sci 25:183
6. Floyd RA, Schneider JE Jr, Dittmer DP (2004) Antiviral Res 61:141
7. Pons OR, Gregorio DM, Mateo JVG, Calatayud JM (2001) Anal Chim Acta 438:149
8. Chatterjee D, Mahata A (2001) Appl Catal B Environ 33:119
9. Ganesan V, John SA, Ramaraj R (2001) J Electroanal Chem 502:167
10. Jana AK (2000) J Photochem Photobiol A Chem 132:1
11. Ensafi AA, Kazemzadeh A (2002) Microchem J 72:193
12. Tatikolov AS, Costa SMB (2004) Biophys Chem 107:33
13. Choudhury M, Basu R (1995) J Photochem Photobiol A Chem 85:89
14. Gessner F, Schimitt CC, Neumann MG (1994) Langmuir 10:3749
15. Cione APP, Neumann MG, Gessner F (1998) J Colloid Int Sci 198:106
16. (a) Pariser R, Parr RG (1953) J Chem Phys 21:466; (b) Pople JA (1953) Trans Faraday Soc 49:1375
17. Del Bene J, Jaffe HH (1968) J Chem Phys 48:1807
18. Ridley JE, Zerner MC (1973) Theor Chim Acta 32:111
19. (a) Zerner MC, Lowe GH, Kirchner RF, Mueller-Westerhoff UT (1980) J Am Chem Soc 102:589; (b) Anderson WP, Edwards WD, Zerner MC (1986) Inorg Chem 25:2728; (c) Bacon AD, Zerner MC (1979) Theo Chim Acta 53:21; (d) Ridley JE, Zerner MC (1976) Theo Chim Acta 42:223; (e) Thompson MA, Zerner MC (1991) J Am Chem Soc 113:8210; (f) Zerner MC, Correa de Mello P, Hehenberger M (1982) Int J Quant Chem 21:251; (g) Hanson LK, Fajer J, Thompson MA, Zerner MC (1987) J Am Chem Soc 109:4728
20. (a) Adachi M, Nakamura S (1991) Dyes Pigments 17:287; (b) Adachi M, Murata Y, Nakamura S (1993) J Am Chem Soc 115:4331; (c) Adachi M, Murata Y, Nakamura S (1995) J Phys Chem 99:14240; (d) Yates PC, Patel B (1994) J Mol Struct (Theochem) 315:117; (e) Lupan L (1998) Rev Roumaine Chimie 43:671
21. Guillaumont D, Nakamura S (2000) Dyes Pigment 46:85
22. Tomasi J, Persico M (1994) Chem Rev 94(7):2027
23. (a) Cancès E, Mennucci B, Tomasi J (1997) J Chem Phys 107:3032; (b) Mennucci B, Cancès E, Tomasi J (1997) J Phys Chem B 101:10506; (c) Cancès E, Mennucci B (1998) J Math Chem 23:309
24. (a) Miertus S, Scrocco E, Tomasi J (1981) Chem Phys 55:117; (b) Cammi R, Tomasi J (1995) J Comp Chem 16:1449
25. Dewar MJ, Zoebisch EG, Healy EF, Stewart JJP (1985) J Am Chem Soc 107:3902
26. (a) Hohenberg P, Kohn W (1964) Phys Rev 136:B864; (b) Kohn W, Sham LJ (1965) Phys Rev 140:A1133; (c) Salahub DR, Zerner MC (1989) The challenge of d and f electrons. ACS, Washington; (d) Parr RG, Yang W (1989) Density-functional theory of atoms and molecules. Oxford University Press, Oxford
27. (a) Stratmann RE, Scuseria GE, Frisch MJ (1998) J Chem Phys 109:8218; (b) Bauernschmitt R, Ahlrichs R (1996) Chem Phys Lett 256:454; (c) Casida ME, Jamorski C, Casida KC, Salahub DR (1998) J Chem Phys 108:4439
28. Frisch MJ, Trucks GW, Schlegel HB, Scuseria GE, Robb MA, Cheeseman JR, Montgomery JA Jr, Vreven T, Kudin KN, Burant JC, Millam JM, Iyengar SS, Tomasi J, Barone V, Mennucci B, Cossi M, Scalmani G, Rega N, Petersson GA, Nakatsuji H, Hada M, Ehara M, Toyota K, Fukuda R, Hasegawa J, Ishida M, Nakajima T, Honda Y, Kitao O, Nakai H, Klene M, Li X, Knox JE, Hratchian HP, Cross JB, Adamo C, Jaramillo J, Gomperts R, Stratmann RE, Yazyev O, Austin AJ, Cammi R, Pomelli C, Ochterski JW, Ayala PY, Morokuma K, Voth GA, Salvador P, Dannenberg JJ, Zakrzewski VG, Dapprich S, Daniels AD, Strain MC, Farkas O, Malick DK, Rabuck AD, Raghavachari K, Foresman JB, Ortiz JV, Cui Q, Baboul AG, Clifford S, Cioslowski J, Stefanov BB, Liu G, Liashenko A, Piskorz P, Komaromi I, Martin RL, Fox DJ, Keith T, Al-Laham MA, Peng CY, Nanayakkara A, Challacombe M, Gill PMW, Johnson B, Chen W, Wong MW, Gonzalez C, Pople JA (2003) Gaussian 03, Development Version, Gaussian Inc., Pittsburgh
29. (a) Ditchfield R, Hehre WJ, Pople JA (1971) J Chem Phys 54:724; (b) Hehre WJ, Ditchfield R, Pople JA (1972) J Chem Phys 56:2257; (c) Hariharan PC, Pople JA (1974) Mol Phys 27:209; (d) Gordon MS (1980) Chem Phys Lett 76:163; (e) Hariharan PC, Pople JA (1973) Theor Chim Acta 28:213; (f) Blaudeau JP, McGrath MP, Curtiss LA, Radom L (1997) J Chem Phys 107:5016; (g) Francl MM, Pietro WJ, Hehre WJ, Binkley JS, DeFrees DJ, Pople JA, Gordon MS (1982) J Chem Phys 77:3654; (h) Binning RC Jr, Curtiss LA (1990) J Comp Chem 11:1206; (i) Rassolov VA, Pople JA, Ratner MA, Windus TL (1998) J Chem Phys 109:1223; (j) Rassolov VA, Ratner MA, Pople JA, Redfern PC, Curtiss LA (2001) J Comp Chem 22:976; (k) Clark T, Chandrasekhar J, Spitznagel GW, Schleyer PVR (1983) J Comp Chem 4:294; (l) Frisch MJ, Pople JA, Binkley JS (1984) J Chem Phys 80:3265
30. (a) Lee C, Yang W, Parr RG (1988) Phys Rev B 37:785; (b) Miehlich B, Savin A, Stoll H, Preuss H (1989) Chem Phys Lett 157:200; (c) Becke AD (1993) J Chem Phys 98:5648
31. (a) Cammi R, Mennucci B (1999) J Chem Phys 110:9877; (b) Cammi R, Mennucci B, Tomasi J (2000) J Phys Chem A 104:5631
32. Caricato M, Mennucci B, Tomasi J (2004) J Phys Chem A 108:6248
33. (a) Cammi R, Tomasi J (1995) Int J Quantum Chem: Quantum Chem Symp 29:465; (b) Mennucci B, Cammi R, Tomasi J (1998) J Chem Phys 109:2798; (c) Ingrosso F, Mennucci B, Tomasi J (2003) J Mol Liquids 108:21
34. Bondi A (1964) J Phys Chem 68:441